Environ. Sci. Technol. **2006**, *40,* 2805−2811

Ambient Particulate Matter Exhibits Direct Inhibitory Effects on Oxidative Stress Enzymes

CHRISTOS HATZIS,[‡] JOHN J. GODLESKI,[†] BEATRIZ GONZÁLEZ-FLECHA,[†] JACK M. WOLFSON,[†] AND PETROS KOUTRAKIS*,[†]

Department of Environmental Health, Harvard School of Public Health, Boston, Massachusetts 02215, and Nuvera Biosciences, Incorporated, 400 West Cummings Park-Suite 5350, Woburn, Massachusetts 01801

A primary mechanistic hypothesis by which ambient air particles have a significant negative impact on human health is via the induction of pulmonary inflammatory responses mediated through the generation of reactive oxygen species (ROS). Development of a biosensor for the assessment of particulate ROS activity would be a significant advance in air pollution monitoring. The objective of this study was to evaluate whether air particulates interact directly with protective enzymes involved in oxidative stress responses. We performed enzyme activity assays on four enzymes involved in oxidative stress responses (Cu/Zn superoxide dismutase, Mn superoxide dismutase, glutathione peroxidase, and glutathione reductase) in the presence of particles of varying toxicities and found distinctive inhibition patterns. On the basis of these findings, we suggest a strategy for an enzyme bioassay that could be used to assess the potential of particles to generate ROS-induced responses.

Introduction

Numerous epidemiological studies have linked particle exposures to increased risk of respiratory and cardiovascular morbidity and mortality (*1*). Although the underlying biological mechanisms mediating these effects are not completely understood, there is evidence that inhaled particles penetrate deep into the lung where they interact with pulmonary cells and may trigger a chain of inflammatory and systemic reactions (*2*−*7*). Of increasing concern is the ability of airborne particulate matter (PM) to cause DNA damage to somatic cells, potentially leading to cancer (*8*, *9*). Recent studies have suggested that certain PM-induced DNA mutations could be passed on to the next generation of lab mice exposed to particulate air pollution, presumably through genetic changes in the male mouse germ cells (*10*, *11*), implying potential genetic risks of particle exposures on human health.

It is well-established that PM exhibits oxidant properties that can cause oxidative tissue damage (*12*). The oxidative capacity of PM is typically attributed to constituent transition metals and quinones that are capable of producing reactive oxygen species (ROS) by catalyzing Fenton-type reactions and through redox recycling mechanisms (*13*). However, other PM characteristics such as organic carbon, silica content (*14*), and total surface area (*15*) appear to independently contribute to the overall toxicity. Irrespective of the mechanistic details, the initial biological response to PM seems to be mediated primarily through pro-inflammatory oxidative stress reactions involving ROS (reviewed in ref *12*). A recent study from our laboratory has provided direct evidence that PM indeed induces higher intracellular ROS concentrations in vivo (*16*). The intracellular accumulation of ROS then elicits an oxidative stress response signal that activates the transcription of oxidative-stress responsive transcription factors leading to the translation of enzymes involved in the removal of ROS, including superoxide dismutase (SOD), glutathione reductase (GSR), glutathione peroxidase (GPX), and catalase (*17*).

The oxidative capacity of different types of PM and the biological responses that these particles elicit vary considerably with the composition and physical characteristics of particles and, to a lesser extent, with the total particle mass (*16*, *18*, *19*). Therefore, from the air quality perspective, it would be advantageous to include measurements of the particle oxidative potential in addition to those for particle mass. Several of the enzymes involved in oxidative stress response have known sensitivities to certain transition metals (*13*); however, it has not been shown whether PM directly inhibits their activity. The present study was designed to evaluate the following questions: (i) do surrogates of ambient particles directly inhibit the activity of enzymes involved in biological toxic response; and (ii) are these inhibitory profiles specific enough to allow discrimination of PMs with varying toxicity?

Experimental Procedures

Particle Surrogates. Particle surrogates (PSs) have been used extensively in experimental studies that aim to characterize the toxicity of PM or to test monitoring instrumentation. For this study, we selected a panel of three PSs with well-characterized in vivo toxicity profiles that cover a broad range of toxicities and physical−chemical characteristics. Residual oil fly ash (ROFA) particles were collected at a Boston area oil fired power plant. These have been used in published studies from our laboratory and others (*20*−*22*). ROFA particles have known pulmonary toxicity, which is mainly due to high levels of constituent alkali and transition metals, including Al, Fe, and Ni in the water-soluble fraction and Fe, V, and Al in the insoluble fraction (*23*, *24*). ROFA was the most toxic PS among the three surrogates studied. The National Institute of Standards and Technology (NIST) urban particulate matter (SRM 1648) contains several metals, mainly Al, Fe, and K, and high levels of silica and sulfate (*25*). Most of the transition metals are present in the oxidized form as oxides or sulfates. The NIST SRM 1648 particles generate ROS in in vitro cell-free assays (*26*). This PS type represents standard urban ambient particles with moderate toxicity. Finally, the silicate-rich Mt. St. Helen's volcanic ash (MSHA) particles were used as chemically inert PS of relatively low toxicity (*27*). MSHA particles, obtained from the Bates Ridge site in Missoula, MT, were size-fractionated by elutriation. These particles have been used previously in studies by our group (*24*, *27*).

Working stocks were prepared in deionized water at concentrations of 1 and 10 mg/mL. The suspensions were sonicated for 30 s and stored at 4 °C at least for 24 h prior to use. The suspensions were sonicated again immediately prior to use in the assays. In preliminary tests, the surfactant

* Corresponding author e-mail: petros@hsph.harvard.edu.
[†] Harvard School of Public Health.
[‡] Nuvera Biosciences.

10.1021/es0518732 CCC: $33.50 © 2006 American Chemical Society
Published on Web 03/16/2006

Triton X-100 (Sigma) was dissolved in deionized water prior to the addition of the particles to help disperse the particles. However, since its benefit was rather marginal, this surfactant was not used in the final assay.

Enzyme Panel Selection. The enzymes in the test panel were selected on the basis of their participation in oxidative stress response pathways and sensitivity to metals. Previous microarray gene expression studies from our group using rat alveolar macrophages demonstrated that exposure to concentrated ambient particles induced the expression of genes that encode for enzymes involved in oxidative stress response (*18*). Genes encoding for the enzymes Cu/Zn superoxide dismutase (SOD), glutathione reductase, and thioredoxin reductase were overexpressed by at least 3-fold. Furthermore, the activity of Cu/Zn SOD doubled in the heart of rats that were exposed in vivo to concentrated ambient particles (CAPs) (*16*).

On the basis of the previous considerations, four enzymes were selected for the panel: (i) Cu/Zn superoxide dismutase (Cu/ZnSOD), a cytoplasmic metalloenzyme that catalyzes the dismutation of superoxide ion to molecular oxygen and hydrogen peroxide and thus is a critical component of the oxidative stress defense mechanism; (ii) Mn superoxide dismutase (MnSOD), a mitochondrial isoenzyme with the same function as stated previously but with potentially different sensitivity to soluble metals; (iii) glutathione peroxidase (GPx), an enzyme (containing selenocysteine in the active site) that catalyzes the reduction of hydroxyperoxides, including hydrogen peroxide, using glutathione as the reducing substrate, and therefore is another key component of the defense mechanism against oxidative stress; and (iv) glutathione reductase (GR), a flavaprotein (containing a redox-active disulfide bond at its active site) that catalyzes the NADPH-dependent reduction of oxidized glutathione and therefore is essential for maintaining the levels of reduced glutathione in the cell.

Enzymatic Assays. Assay kits in the 96-well format from Cayman Chemical (Ann Arbor, MI) were used in this study (Superoxide Dismutase Assay Kit, cat# 706002; Glutathione Reductase Assay Kit, cat# 73202; and Glutathione Peroxidase Assay Kit, cat#73102). The MnSOD enzyme was purchased from Sigma and was assayed using the same assay kit. All assays were performed according to the protocols provided with the kits, with the only exception that about 10 μL of sample buffer was substituted with the particle suspension prepared as described previously, thereby keeping the same total assay volume in each well. Absorbance at 450 and 570 nm was measured on a Umax microplate reader (Molecular Devices), and absorbance at 340 nm was measured on a Spectrafluor Plus (Tecan).

Nonspecific Protein Absorption. The enzymatic assay results could have been biased by nonspecific absorption of the enzymes onto particles. To evaluate the extent of nonspecific protein absorption, the fraction of free protein that remained in the suspension after incubation in particle suspensions at assay conditions was measured using the Bradford assay in a 96-well format (Bradford reagent purchased from Sigma). Five microliters of concentrated protein stock (MnSOD) was added to all wells followed by 10 μL of the concentrated particle suspension stock or 10 μL of the SOD assay sample buffer (from the SOD Assay Kit) for the control wells. Then, 250 μL of the Bradford reagent was added to all wells to start the reaction. The microplate was placed on an orbital shaker and allowed to mix for 30 s, followed by 10 min incubation at room temperature and subsequent centrifugation at 1000*g* for 90 s to remove the particles carrying the absorbed protein. Finally, 100 μL of the supernatant was transferred to a fresh plate, and absorbance at 570 nm was measured using a Umax reader (Molecular Devices). The protein−dye complex of the Bradford assay was stable for only 60 min, and therefore, all steps had to be completed within this time frame. The fraction of absorbed protein was estimated from the slopes of the standard curves (absorbance vs protein concentration) in the presence or absence of particles.

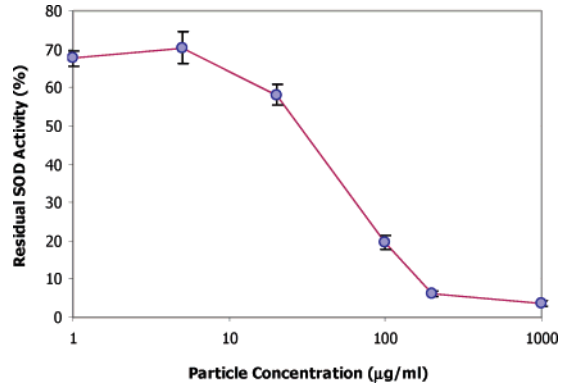

FIGURE 1. Dose−response curve for NIST particles in 0.1% Triton X-100 on Cu/Zn SOD activity. The bias-adjusted mean residual activity and standard deviation were estimated using 1000 bootstrap replicates of the original data (n = 4 wells per assay).

Data Analysis and Statistics. Multiple replicate wells per treatment (two to six wells) were used in all assays. Bootstrap means and standard deviations (*28*) were calculated for all the enzymatic activity measurements. The bias-adjusted means (instead of the observed averages) were typically reported, and comparisons between treatments were based on the bias-corrected and adjusted (BCa) 95% confidence intervals. The resampling estimates were based on 1000 bootstrap replications using the software S-Plus 6.1 (Insightful, Seattle, WA). The bootstrap estimation of the residual activity was carried out as follows. For each particle type and concentration combination, four samples were assayed: a control without any enzyme or particles (S0), a control with enzyme but without particles (Se), a control with particles but no enzyme (Sp), and the sample with enzyme and particles (S). Each of these four samples was assayed in replicate on the multiwell plate (two to six replicates). The activity of the enzyme in the absence of particles, E_0, was quantified by the ratio of absorbances A_{S0}/A_{Se} and the corresponding activity in the presence of particles, E_S, by the ratio A_{Sp}/A_S. Finally, the residual activity was estimated as the ratio $(E_S/E_0) \times 100$ (activity %). Because of this sequence of calculations, it is not possible to calculate directly the accuracy of the final estimate of residual activity from the replicated readings of absorbance. We used bootstrap to accomplish this by sampling the replicated absorbances several times (up to 1000) with replacement, and from each sample we estimated the residual activity. The bias and bias-corrected confidence intervals were then estimated from the bootstrap-generated distribution of the estimate of residual activity.

Results

Effect of Particles on Enzyme Activity−Assay Optimization. Initial tests were conducted to evaluate potential interference of the NIST particles with the Cu/ZnSOD enzymatic activity assay and to establish the effective concentration range of PMs in the particle inhibition assays. The activity of the control sample (without particles or surfactant) was 0.25 U/mL, which is at the upper end of the linear range of the assay. Figure 1 shows the effect of NIST particles in 0.1% Triton X-100 on the residual activity of Cu/ZnSOD, suggesting an effective inhibitory range between 10 and 100 μg/mL particles. Less than 5% of the initial Cu/ZnSOD activity

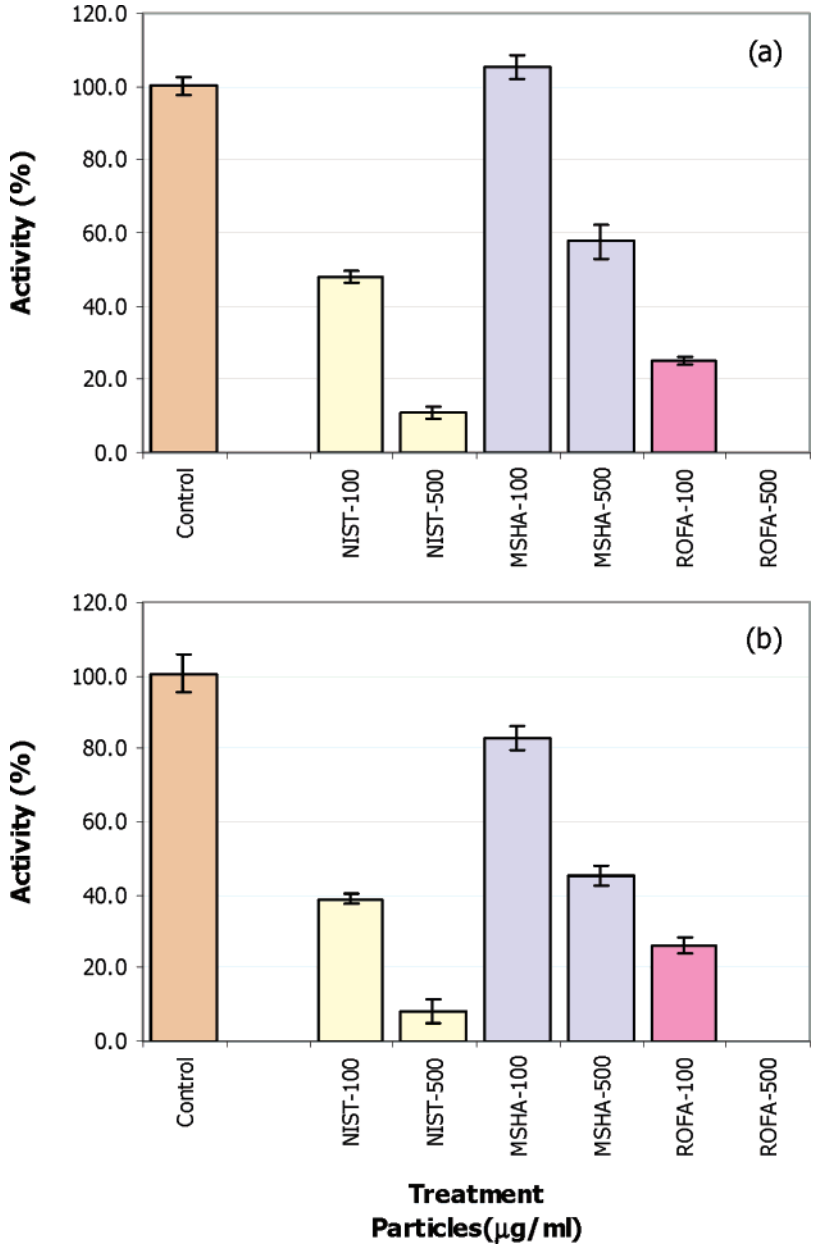

FIGURE 2. Effect of PM type and concentration on the activity of Cu/ZnSOD (a) and MnSOD (b). The bootstrap bias-adjusted means and standard deviations were based on 1000 bootstrap replicates of the original data ($n = 5$ wells per assay).

remained above 200 μg/mL. The addition of 0.1% Triton X-100 in the assay caused a small but noticeable inhibitory effect (the 95% bootstrap confidence intervals of residual activity in the presence of 200 μg/mL NIST particles with or without addition of Triton were [4.6−7.6] and [7.4−12.7], respectively), and therefore, it was omitted from further assays.

Inhibition Profiles of Oxidative Stress Enzymes by Particle Surrogates. Particles without a surfactant agent were added to the assay at final concentrations of 100 and 500 μg/mL. Results from the assays on Cu/Zn SOD and Mn SOD enzymes are shown in Figure 2. In both cases, the control treatment consisted of the corresponding enzyme at 0.15 U/mL, which falls at the middle of the linear range for the assay, with no particles added. The standard curve for each enzyme was determined from a range of standards according to the assay protocol, using replicate wells in the same microplate to ensure consistency within each experiment.

The effects of the particle type and concentration appear to be similar for both SODs. The NIST particles reduced the activity of both enzymes by about 50% when present at 100 μg/mL and by more than 90% at a level of 500 μg/mL. The ROFA particles were clearly more active, eliciting 75 and 100% inhibition of the enzymatic activities when present at 100 and 500 μg/mL, respectively. While the most inert PS, MSHA particles, were the least inhibitory and did not reduce the activity of Cu/Zn SOD at 100 μg/mL, they did show a small but significant inhibitory effect on the activity of Mn SOD (the 95% bootstrap confidence interval of residual Mn SOD activity was [76.3, 88.9]).

The effects on the remaining two enzymes on the panel are shown in Figure 3. Overall, glutathione reductase (GR) appears to be less sensitive to particle-induced inhibition, as compared to the SODs. The MSHA particles had no apparent effect on GR activity, whereas the ROFA particles at 500 μg/mL caused a 74% inhibition, as compared to complete inhibition of SOD at the same concentration. Glutathione peroxidase (GPx) appeared to be more sensitive to particle effects as compared to GR, and its inhibition profile was similar to those of the SOD enzymes. A distinctive difference, however, is that GPx appears to be less sensitive

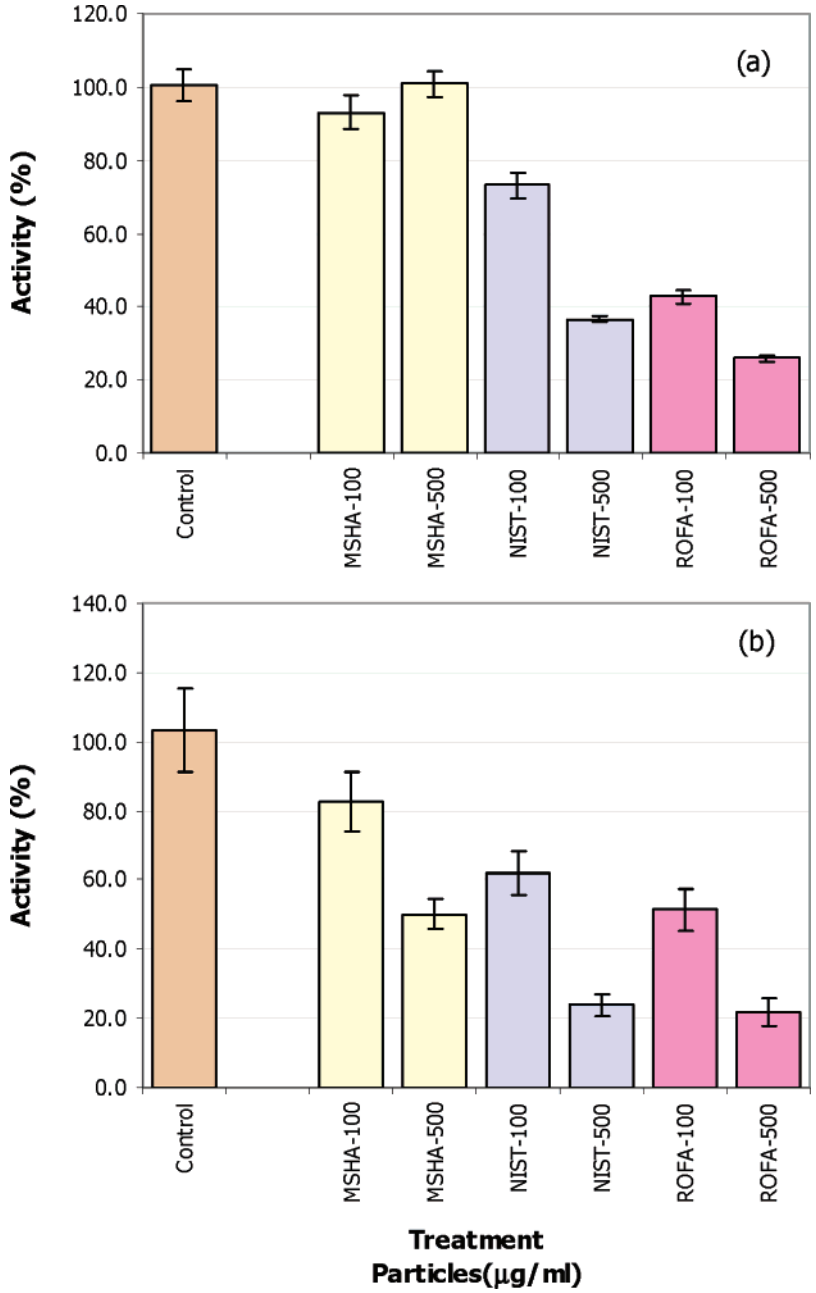

FIGURE 3. Effect of PM type and concentration on the activity of glutathione reductase (a) and glutathione peroxidase (b). The bootstrap bias-adjusted means and standard deviations were based on 1000 bootstrap replicates of the original data ($n = 6$ wells per assay).

to the ROFA particles as compared to the other enzymes in the panel, and this could provide a basis for discriminating ambient air particles with composition similar to ROFA particles from other types of ambient particles.

Nonspecific Effects on Enzymatic Activity. The concentration-dependent effects on the activity of the oxidative stress response enzymes exhibited by the PSs are probably attributable to increased levels of soluble components released by the particles. However, nonspecific absorption of the enzymes on the particles could cause a similar concentration-dependent reduction in total activity by decreasing the amount of free enzyme that remains available for the enzymatic assay. Nonspecific absorption was quantified as the fraction of protein (MnSOD) that remained in suspension in particle-containing suspensions relative to particle-free controls. This fraction was estimated over a range of protein concentrations from the ratio of the corresponding standard lines (absorbance vs protein concentration) as described in the Experimental Procedures.

TABLE 1. Absorption of MnSOD on Different PS Types[a]

particle type	concentration (μg/mL)	free protein (%)			
		mean	SD	BCa-2.5%	BCa-97.5%
MSHA	100	98.7	5.6	90.1	112.1
MSHA	500	89.9	8.4	75.6	108.6
NIST	100	93.5	5.0	85.6	105.2
NIST	500	74.0	6.2	62.9	85.9
ROFA	100	67.4	11.9	45.9	86.7
ROFA	500	7.7	15.1	−17.1	42.2

[a] Statistics estimated based on 1000 bootstrap replicates of the original data. The slopes of the standard curves were estimated in duplicate ($n = 2$ wells per treatment) using four protein concentrations (0, 0.1, 0.4, and 0.8 mg/mL) per particle type/concentration combination shown in the table.

Table 1 summarizes the results on protein absorption for the different PSs. The MSHA particles did not cause any

significant reduction in the free protein (the 95% bootstrap confidence intervals for both concentrations contain the value of 100%), and the effect was similar for NIST particles at 100 μg/mL. However, the NIST particles at 500 μg/mL and the ROFA particles at the lower concentration absorbed about 30% of the protein, while a suspension of 500 μg/mL ROFA particles removed practically all the protein. This last result, however, should be interpreted with caution due to the wide 95% confidence interval (see Table 1), which indicates problems with reproducibility and potential interference of the ROFA particles with the protein assay. Overall, although some PSs showed sizable nonspecific protein absorption, this effect alone could not explain the magnitude of inhibition in enzymatic activity observed. Therefore, PSs appear to affect not only the concentration of the free enzyme but also the specific activity of the enzymes as measured in this study. Obviously, the above conclusion assumes that the nonspecific absorption of all enzymes in the panel will be similar to the absorption of MnSOD that was measured in this study.

Discrimination of Particle Surrogates Based on Enzyme Inhibition Profiles. An objective of this study was to evaluate whether the inhibitory signatures of the various PSs are specific enough to allow discrimination of PSs with different toxicity profiles. For this purpose, it is useful to summarize the particle inhibition assay results by PSs, as shown in Figure 4. It then becomes clear that the different PSs exhibit different inhibitory patterns on the four enzymes in the panel. Overall, MSHA particles appear to be the least inhibitory, followed by the NIST particles, which were moderately inhibitory especially against the SOD enzymes. The ROFA particles were the most inhibitory at both concentrations tested in this study. The previous order of inhibition capacity of the different PSs is consistent with their in vivo toxicity.

To help elucidate the differences in the inhibitory signatures associated with the different PSs, we performed principal component analysis (PCA) on the residual activity data shown in Figure 4. The activity scales of the four enzymes in the panel form a 4-D space, and each of the eight data points (four types of PS $\times$ 2 concentrations) can be represented by a 4-D vector in this space. PCA finds orthogonal projections of the original data vectors onto spaces of lower dimensionality, with the direction of the new projections selected to maximize the variance contained in the data along those directions. Thus, by keeping the first two orthogonal directions, the 4-D vectors of inhibition patterns can be visualized in a 2-D plot.

Figure 5 shows the PCA biplot of the enzyme inhibition data obtained in this study. The original data points are represented as arrows starting at the origin with their directions and lengths determined by the loading factors or relative contributions of the four enzymes in the panel. Areas of different toxicity can be identified on the biplot: a low toxicity area in the lower half of the plot spanned by the MSHA particles, a high toxicity area in the upper half of the plot spanned by the ROFA particles, and a moderate toxicity area spanned by the NIST particles that falls between the other two. The projections of both concentrations of the same PS are close to each other, indicating that the inhibition signatures reflect particle-specific characteristics rather than nonspecific concentration-dependent effects. One notable exception was the MSHA particles that had a more toxic profile at 500 μg/mL, and this cannot be explained on the basis of nonspecific absorption.

Discussion

Inhaled particles induce adaptive biological responses in lung cells, and this principle could form the basis for an in vitro cell-based assay strategy for assessing the oxidative potential of PM. Although cell-based biosensors are attractive in principle, their practical application is hindered by challenges

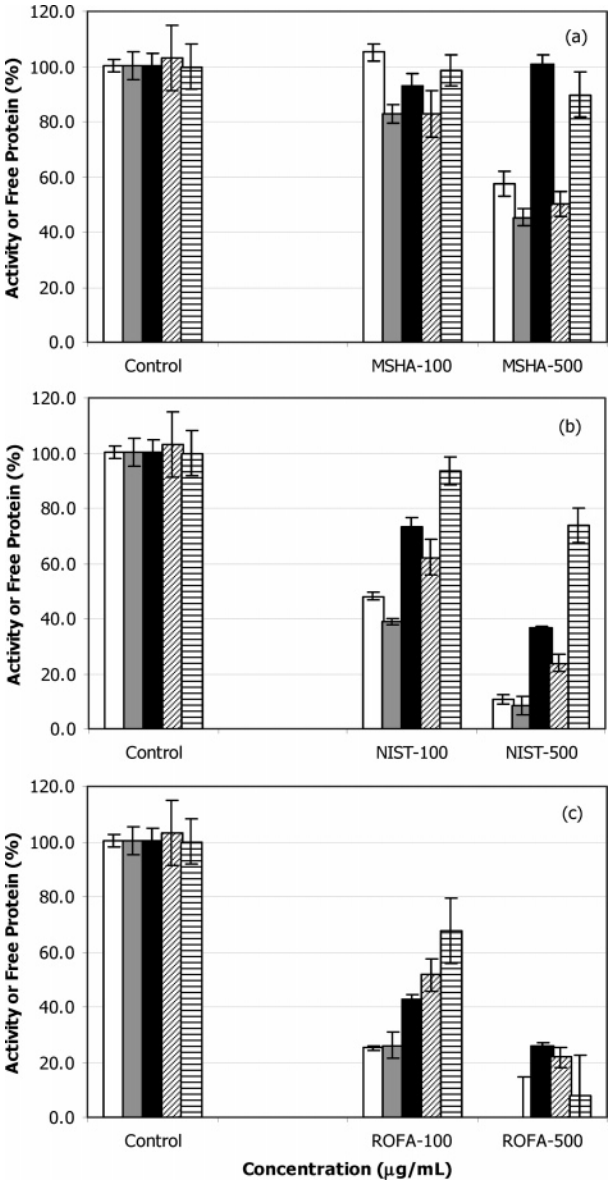

FIGURE 4. Enzyme inhibition signatures for the different particle surrogates: (a) MSHA particles, (b) NIST particles, and (c) ROFA particles. Bars show percent residual enzymatic activity (Cu/ZnSOD: white; Mn/SOD: gray; GR: black bar; and GPx: upward diagonal pattern) or percent free protein (horizontal pattern). Error bars were computed as described in previous figures.

involved with the maintenance of the living component active for prolonged periods of time and in ensuring compatibility with the other components of the sensor (*29*, *30*). Cell-free systems such as bioaffinity sensors, enzyme biosensors, and transmembrane sensors offer a compromise with narrower detection capabilities but superior sensor stability and therefore are preferable for near term applications (*31*).

It is reasonable to expect that the activity of certain enzymes, specifically metalloenzymes and antioxidant enzymes, would be directly modulated by the components of the PM and that such enzymes would exhibit differential sensitivities to the bioavailable metal ions. This hypothesis, if proven true, can form the basis for a cell-free, enzyme biosensor for determining the oxidative potential of PM. Along these lines, Aust and colleagues (*32*) proposed an in vitro cell-free assay to quantify the production of ROS by transition metals and thus to determine the potential of particles of unknown composition to generate ROS-mediated inflammatory response. The proposed assay is based on the metal

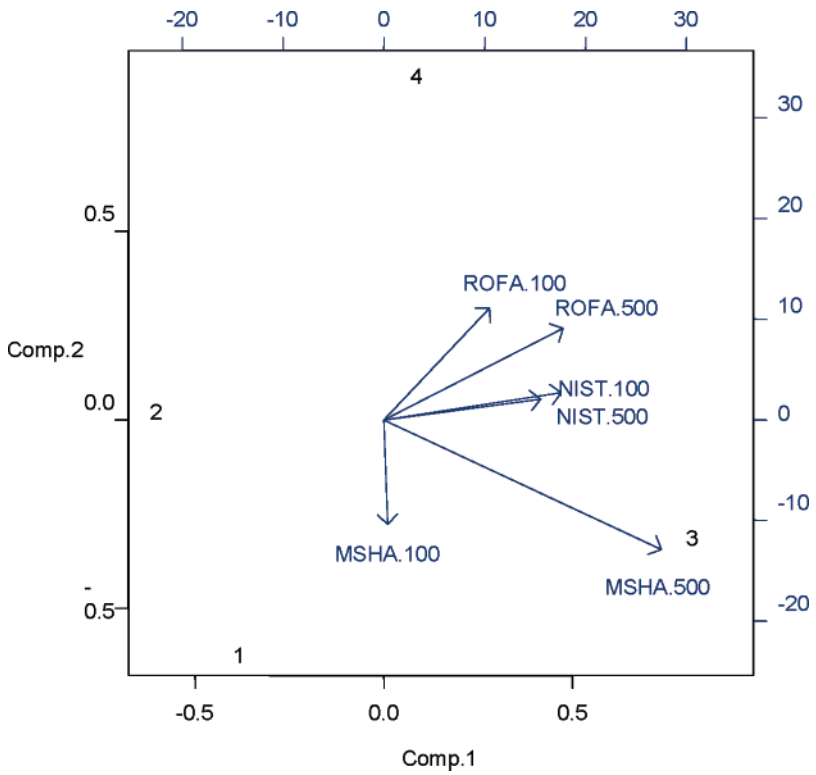

FIGURE 5. Principle component biplot of the enzyme inhibition data by particle surrogates. Particle suspensions of different types and concentrations are represented by arrows.

catalyzed production of a hydroxyl free radical that can be detected spectrophotometrically. Since ROS can be generated through different reaction mechanisms (e.g., redox reactions catalyzed by transition metals or redox recycling for the organic components of the particles), ideally an assay or biosensor for the ROS potential of particles should not be tied to a specific chemistry, which is a limitation of the approach mentioned previously.

An electron spin resonance method has been recently optimized for the determination of ROS-generating capacity of PM collected onto filters (*33*). This method has high selectivity and sensitivity for the determination of free radicals; however, it is much more complex and requires technology and expertise not available in many laboratories. Additionally, the assay is based on the addition of reducing agents to the filters, which will favor production of ROS via redox cycling mechanisms and may bias the results to show organic compounds as the main sources of ROS.

The reaction of dichlorofluorescein (DCFH) with peroxides has been developed into a widely used assay to quantify intracellular hydroperoxides, including H_2O_2. This method has been also suggested for measuring ROS in cell-free systems. Free DFCH is oxidized by peroxides, yielding fluorescent DCF that can be easily detected by fluorometry, fluorocytometry, or fluorescence microscopy. While this assay is easy to perform, it lacks specificity since DCFH can be oxidized not only by H_2O_2 but also by organic peroxides (*34*).

In this study, we demonstrated for the first time that particles interact directly and inhibit in vitro the specific activity of enzymes involved in oxidative stress response. Moreover, for the different PS types tested, the inhibitory capacity of the particulates on the selected enzymes correlates with the in vivo toxicity of the particles (MSHA < NIST < ROFA). Our findings suggest that the potential to generate oxidative stress of ambient particles may be determined, at least in principle, on the basis of the pattern of inhibition of the enzymatic activity of a carefully selected panel of enzymes. A particle sample of unknown composition and oxidative stress potential could be assayed at 100 μg/mL in the microplate format, which requires only small amounts of particles and reagents. The residual activity vector would then be multiplied by the PCA loading factors and mapped onto the 2-D biplot. The toxic potential of the unknown specimen will then be determined based on its proximity with samples of known toxicity. The resolving ability of the system could be potentially improved by adding to the panel enzymes that are sensitive to other metals, such as metallothionein that binds heavy metals or ferritin that binds iron ions. Further testing and validation of the specificity and sensitivity of the current system to concentrated ambient particles collected from an urban site is the planned next step in this study.

Acknowledgments

Although the research in this article has been funded wholly or in part by the U.S. Environmental Protection Agency through grant #R827353 to the Harvard School of Public Health, it has not been subjected to the Agency's required peer and policy review and therefore does not reflect the views of the Agency and no official endorsement should be inferred. Dr. Andrei Sarna-Wojnicki of the U.S. Geological Service provided the Mt. St. Helen's Ash sample used in this study.

Literature Cited

(1) Pope, C. A., III; Burnett, R. T.; Thun, M. J.; Calle, E. E.; Krewski, D.; Ito, K.; Thurston, G. D. Lung cancer, cardiopulmonary mortality, and long-term exposure to fine particulate air pollution. *J. Am. Med. Assoc.* **2002**, *287*, 1132−1141.

(2) Li, N.; Venkatesan, M. I.; Miguel, A.; Kaplan, R.; Gujuluva, C.; Alam, J.; Nel, A. Induction of heme oxygenase-1 expression in macrophages by diesel exhaust particle chemicals and quinones via the antioxidant-responsive element. *J. Immunol.* **2000**, *165*, 3393−3401.

(3) Ghio, A. J.; Suliman, H. B.; Carter, J. D.; Abushamaa, A. M.; Folz, R. J. Overexpression of extracellular superoxide dismutase

decreases lung injury after exposure to oil fly ash. *Am. J. Physiol. Lung. Cell. Mol. Physiol.* **2002**, *283*, L211−218.
(4) Haddad, J. J.; Safieh-Garabedian, B.; Saade, N. E.; Lauterbach, R. Inhibition of glutathione-related enzymes augments LPS-mediated cytokine biosynthesis: involvement of an IkappaB/NF-kappaB-sensitive pathway in the alveolar epithelium. *Int. Immunopharmacol.* **2002**, *2*, 1567−1583.
(5) Lippmann, M.; Frampton, M.; Schwartz, J.; Dockery, D.; Schlesinger, R.; Koutrakis, P.; Froines, J.; Nel, A.; Finkelstein, J.; Godleski, J.; Kaufman, J.; Koenig, J.; Larson, T.; Luchtel, D.; Liu, L. J.; Oberdorster, G.; Peters, A.; Sarnat, J.; Sioutas, C.; Suh, H.; Sullivan, J.; Utell, M.; Wichmann, E.; Zelikoff, J. The U.S. Environmental Protection Agency Particulate Matter Health Effects Research Centers Program: a midcourse report of status, progress, and plans. *Environ. Health Perspect.* **2003**, *111*, 1074−1092.
(6) Koike, E.; Hirano, S.; Shimojo, N.; Kobayashi, T. cDNA microarray analysis of gene expression in rat alveolar macrophages in response to organic extract of diesel exhaust particles. *Toxicol. Sci.* **2002**, *67*, 241−246.
(7) Pradhan, A.; Waseem, M.; Dogra, S.; Khanna, A. K.; Kaw, J. L. Alterations in bronchoalveolar lavage constituents, oxidant/antioxidant status, and lung histology following intratracheal instillation of respirable suspended particulate matter. *J. Environ. Pathol. Toxicol. Oncol.* **2005**, *24*, 19−32.
(8) Upadhyay, D.; Panduri, V.; Ghio, A.; Kamp, D. W. Particulate matter induces alveolar epithelial cell DNA damage and apoptosis: role of free radicals and the mitochondria. *Am. J. Respir. Cell. Mol. Biol.* **2003**, *29*, 180−187.
(9) Soares, S. R.; Bueno-Guimaraes, H. M.; Ferreira, C. M.; Rivero, D. H.; De Castro, I.; Garcia, M. L.; Saldiva, P. H. Urban air pollution induces micronuclei in peripheral erythrocytes of mice in vivo. *Environ. Res.* **2003**, *92*, 191−196.
(10) Samet, J. M.; DeMarini, D. M.; Malling, H. V. Biomedicine. Do airborne particles induce heritable mutations? *Science* **2004**, *304*, 971−972.
(11) Somers, C. M.; McCarry, B. E.; Malek, F.; Quinn, J. S. Reduction of particulate air pollution lowers the risk of heritable mutations in mice. *Science* **2004**, *304*, 1008−1010.
(12) Tao, F.; Gonzalez-Flecha, B.; Kobzik, L. Reactive oxygen species in pulmonary inflammation by ambient particulates. *Free Radical Biol. Med.* **2003**, *35*, 327−340.
(13) Stohs, S. J.; Bagchi, D. Oxidative mechanisms in the toxicity of metal ions. *Free Radical Biol. Med.* **1995**, *18*, 321−336.
(14) Zhang, Z.; Shen, H. M.; Zhang, Q. F.; Ong, C. N. Involvement of oxidative stress in crystalline silica-induced cytotoxicity and genotoxicity in rat alveolar macrophages. *Environ. Res.* **2000**, *82*, 245−252.
(15) Brown, D. M.; Stone, V.; Findlay, P.; MacNee, W.; Donaldson, K. Increased inflammation and intracellular calcium caused by ultrafine carbon black is independent of transition metals or other soluble components. *Occup. Environ. Med.* **2000**, *57*, 685−691.
(16) Gurgueira, S. A.; Lawrence, J.; Coull, B.; Murthy, G. G.; Gonzalez-Flecha, B. Rapid increases in the steady-state concentration of reactive oxygen species in the lungs and heart after particulate air pollution inhalation. *Environ. Health Perspect.* **2002**, *110*, 749−755.
(17) Donaldson, K.; Stone, V. Current hypotheses on the mechanisms of toxicity of ultrafine particles. *Ann. Ist. Super. Sanita* **2003**, *39*, 405−410.
(18) Godleski, J. J.; Clarke, R. W.; Coull, B. A.; Saldiva, P. H.; Jiang, N.-F.; Lawrence, J.; Koutrakis, P. Composition of inhaled urban air particles determines accute pulmonary responses. *Ann. Occup. Hyg.* **2002**, *46* (Supplement 1), 419−424.
(19) Medeiros, N., Jr.; Rivero, D. H.; Kasahara, D. I.; Saiki, M.; Godleski, J. J.; Koutrakis, P.; Capelozzi, V. L.; Saldiva, P. H.; Antonangelo, L. Acute pulmonary and hematological effects of two types of particle surrogates are influenced by their elemental composition. *Environ. Res.* **2004**, *95*, 62−70.
(20) Killingsworth, C. R.; Shore, S. A.; Alessandrini, F.; Dey, R. D.; Paulauskis, J. D. Rat alveolar macrophages express preprotachykinin gene-I mRNA-encoding tachykinins. *Am. J. Physiol.* **1997**, *273*, L1073−1081.
(21) Kodavanti, U. P.; Hauser, R.; Christiani, D. C.; Meng, Z. H.; McGee, J.; Ledbetter, A.; Richards, J.; Costa, D. L. Pulmonary responses to oil fly ash particles in the rat differ by virtue of their specific soluble metals. *Toxicol. Sci.* **1998**, *43*, 204−212.
(22) Wellenius, G. A.; Saldiva, P. H.; Batalha, J. R.; Krishna Murthy, G. G.; Coull, B. A.; Verrier, R. L.; Godleski, J. J. Electrocardiographic changes during exposure to residual oil fly ash (ROFA) particles in a rat model of myocardial infarction. *Toxicol. Sci.* **2002**, *66*, 327−335.
(23) Dreher, K. L.; Jaskot, R. H.; Lehmann, J. R.; Richards, J. H.; McGee, J. K.; Ghio, A. J.; Costa, D. L. Soluble transition metals mediate residual oil fly ash induced acute lung injury. *J. Toxicol. Environ. Health* **1997**, *50*, 285−305.
(24) Lewis, A. B.; Taylor, M. D.; Roberts, J. R.; Leonard, S. S.; Shi, X.; Antonini, J. M. Role of metal-induced reactive oxygen species generation in lung responses caused by residual oil fly ash. *J. Biosci.* **2003**, *28*, 13−18.
(25) Huggins, F. E.; Huffman, G. P.; Robertson, J. D. Speciation of elements in NIST particulate matter SRMs 1648 and 1650. *J. Hazard. Mater.* **2000**, *74*, 1−23.
(26) Ball, J. C.; Straccia, A. M.; Young, W. C.; Aust, A. E. The formation of reactive oxygen species catalyzed by neutral, aqueous extracts of NIST ambient particulate matter, and diesel engine particles. *J. Air Waste Manage. Assoc.* **2000**, *50*, 1897−1903.
(27) Savage, S. T.; Lawrence, J.; Katz, T.; Stearns, R. C.; Coull, B. A.; Godleski, J. J. Does the Harvard/U.S. Environmental Protection Agency Ambient Particle Concentrator change the toxic potential of particles? *J. Air Waste Manage. Assoc.* **2003**, *53*, 1088−1097.
(28) Efron, B.; Tibshirani, R. J. *An Introduction to the Bootstrap*; Chapman and Hall/CRC: Boca Raton, FL, 1993.
(29) Bousse, L. Whole cell bioscensors. *Sens. Actuators, B* **1996**, *34*, 270−275.
(30) Rudolph, A. S.; Reasor, J. Cell and tissue based technologies for environmental detection and medical diagnostics. *Biosens. Bioelectron.* **2001**, *16*, 429−431.
(31) Ziegler, C.; Gopel, W. Biosensor development. *Curr. Opin. Chem. Biol.* **1998**, *2*, 585−591.
(32) Aust, A. E.; Ball, J. C.; Hu, A. A.; Lighty, J. S.; Smith, K. R.; Straccia, A. M.; Veranth, J. M.; Young, W. C. *Particle Characteristics Responsible for Effects on Human Lung Epithelial Cells*; Research Report 110; Health Effects Institute: Dec 2002.
(33) Briede, J. J.; De Kok, T. M.; Hogervorst, J. G.; Moonen, E. J.; Op Den Camp, C. L.; Kleinjanst, J. C. Development and application of an electron spin resonance spectrometry method for the determination of oxygen free radical formation by particulate matter. *Environ. Sci. Technol.* **2005**, *39*, 8420−8426.
(34) Hinkle, P. C.; Penefsky, H. S.; Racker, E. Partial resolution of the enzymes catalyzine oxidative phosphorylation. XII. The H_2-^{18}O-inorganic phosphate and H_2-^{18}O-adenosine triphosphate exchange reactions in submitochondrial particles from beef heart. *J. Biol. Chem.* **1967**, *242*, 1788−1792.

Received for review September 21, 2005. Revised manuscript received February 6, 2006. Accepted February 7, 2006.

ES0518732